Physical Science International Journal

17(3): 1-9, 2018; Article no.PSIJ.39940
ISSN: 2348-0130

Investigation of Depolarization and Cross Polarization over Ku-band Satellite Links in a Guinea Savanna Location, Nigeria

O. M. Durodola[1*], Ibrahim Aminu[1], J. S. Ojo[2] and M. O. Ajewole[2]

[1]Department of Physics, University of Jos, Nigeria.
[2]Department of Physics, Federal University of Technology, Akure, Nigeria.

Authors' contributions

This work was carried out in collaboration between all authors. Authors OMD, JSO and MOA designed the study as author IA's MSc project, supervised by author OMD. Authors OMD and IA performed the statistical analysis. Author OMD wrote the protocol, while author IA wrote the manuscript, which was corrected and redrafted by author OMD. Authors OMD and JSO managed the analyses of the study. Authors OMD and IA managed the literature searches. All authors read and approved the final manuscript.

Article Information

DOI: 10.9734/PSIJ/2018/39940
Editor(s):
(1) Lei Zhang, Winston-Salem State University, North Carolina, USA.
(2) Roberto Oscar Aquilano, School of Exact Science, National University of Rosario (UNR),Rosario, Physics Institute (IFIR)(CONICET-UNR), Argentina.
Reviewers:
(1) Hermes José Loschi, University of Campinas, Brazil.
(2) Stefano Selleri, University of Florence, Italy.
(3) S. Akhila, BMS College of Engineering, India.
Complete Peer review History: http://www.sciencedomain.org/review-history/23689

Original Research Article

Received 7th January 2018
Accepted 9th March 2018
Published 17th March 2018

ABSTRACT

In communication systems engineering, designers tend to optimize the channel capacity of radio links through frequency re-use by deploying dual independent orthogonally polarized channels in the same frequency band. Such frequency re-use techniques via linear or circular polarization are severely impaired by the interference of cross-polarized signals, because the energy from one polarization is transferred to the other orthogonal region. Depolarization effects on satellite links are described in terms of cross polar discrimination (XPD). The parameters mainly responsible for depolarization due to scattering by oblate spheroid raindrops at Ku-band can be estimated from satellite beacon footprint data. In this paper, data obtained from Ku-band, EUTELSALAT (W4/W7) at a frequency of 12.245 GH_Z and elevation angle of 036° E over Jos, Nigeria (9.9565° N, 8.8583° E, 1258 m) were analyzed. One minute rain rate obtained from rapid response rain gauge was also analyzed alongside the beacon measurements. Consequently, the aforementioned data were

**Corresponding author: E-mail: durotayo@yahoo.com;*

applied to the ITU-R procedure in recommendations 618-12 to estimate XPD due to rain on earth satellite path over the study location. The results show positive values of XPD, the threshold of rain rate of 27 mm/h, while the threshold for co-polar attenuation was found to be 5.6 dB. Also, negative XPD values of about -120 dB obtained indicated that very high incidences of interference and cross-talks could occur in the region; and this could inhibit frequency re-use in the Guinea Savanna region of Nigeria. The overall results obtained provided useful models and thresholds values for radio communication planning in the region.

Keywords: Satellite link; ku-frequency band; depolarization; cross polarization discrimination (XPD).

1. INTRODUCTION

Signal depolarization inhibits the re-use of the frequency of systems with two orthogonal channels for radio communication. Depolarization of satellite signal are caused by the anisotropy of the propagation medium due to the oblateness of raindrops and the melting layer along the earth space propagation path. It is due to the non-spherical symmetry of the raindrops (the top and bottom are flattened), along with their tendency to have a preferred orientation. Depolarization results in cross-talk between two orthogonal polarized channels, transmitted on the same path and frequency band [1]. Signal depolarization inhibits the re-use of the frequency of systems with two orthogonal channels for radio communication. Cross polarization discrimination (XPD) indicates the isolation between the two communication channels with orthogonal polarization (Barclay, 2003) and may be used to measure the effect of depolarisation interference. A high value of XPD implies less interference, while low values of XPD signify high occurrences of interference [2]. The attenuating effects of rain on radio wave propagation may be traced to the microphysical characteristics of rain, such as rain intensity [3], velocity [4], size [5,6], shape [7] and canting angle [8,9] among others. Thus, the amount of rain depolarisation depends on rain rate, signal frequency, size, shape and the relative orientation of the raindrops [10].

1.1 Rain Shape

In [2], Garg and Nayar demonstrated that the shape of the rain-drop varies from spherical to oblate spheroid as it drops from the sky and increases in size. The Raindrop changes shape as it falls from the sky in the presence of drafts and aerodynamic forces. This change in shape is responsible for the depolarisation effect of rain on radio waves as they propagate through the atmosphere. Raindrops less than 1 mm in size are not severely distorted and are therefore modelled as spheres. Oguchi in [11] described the deformation from sphericity with the empirical linear expression:

$$\frac{a}{b} = 1 - \frac{0.41}{4.5} a_0 \quad (1)$$

where, *a* and *b* are the semi-minor and semi-major axes of the raindrop, and a_0 is the equi-volumic radius in mm. Equation (1) was used by [12] to compute various phase shifts, scattering and attenuation parameters of tropical rainfall for frequencies between 1 and 100 GHz in Nigeria.

1.2 Rain Canting Angle

The canting angle of the raindrop is defined as the angle between the major axis of the drop and the local horizontal, denoted as **ξ,** in Fig. 1. It is important for the determination of depolarisation characteristics of rain. Due to aerodynamic

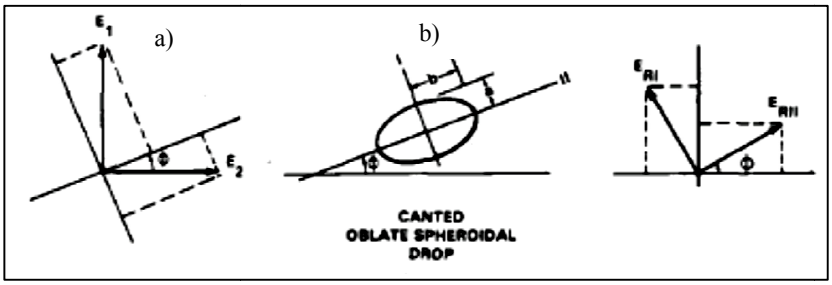

Fig. 1. Canting effect of deformed raindrop [10]: Vector relationship for a depolarizing medium. (a) Co- and cross-polarized waves for linear transmission and (b) Classical model for a canted oblate spherical rain drop

forces around them, non-spherical raindrops wobble, change orientation, and cant away from the vertical and remain on axial orientations different from the vertical, as shown in Fig. 2(c). The canting angle for each raindrop is different and constantly changing as it drops to the ground, varying from -15° to +15° with a mean canting angle of +7°. The distribution in channels is usually modelled as a deterministic or a stochastic distribution with a mean and standard deviation.

The aerodynamic forces are more severe in convective types of rain and so they experience greater depolarisation effects. For modelling rain depolarisation, a canting angle distribution is obtained and the cross-polarization discrimination (XPD) is computed using the mean value of the canting angle.

2. DEPOLARIZATION DUE TO RAIN

The orientation of the line of electric flux in an electromagnetic field is referred to as wave polarization; while a change in the orientation of the electric field of the satellite signal is termed depolarization. Depolarization is induced by rain and multipath propagation. While multipath induced depolarization is limited to terrestrial links, depolarization on satellite paths is caused by rain and ice. The wave while passing through the anisotropic medium experiences attenuation and phase shift that alters its polarization state. Ajewole [12] computed various phase shifts, scattering and attenuation parameters of tropical rainfall for frequencies between 1 and 100 GHz in Nigeria.

During rainfall, as rain gets more intense the size shape and orientation of the raindrop varies as shown in Fig. 2. Consequently, raindrop size distribution (DSD) plays major role in determining satellite signal depolarization [13]. When a radio wave propagates through a non-spherical hydrometeor, the raindrop changes the polarization of the radio wave. Rain depolarisation refers to the deformity experienced by the radio wave signal passing through falling raindrops. Small raindrops are spherical in shape, but as the raindrops grow larger, they become oblate spheroids (flattened underneath by air-resistance opposing the downward movement of the drops). Also, the axis of symmetry of symmetry of the drop is vertical, for vertically falling raindrops, but aerodynamic forces cause some canting and tilting of the drops in a randomized manner as shown in Fig. 2.(a – c).

2.1 Cross-polarization due to Rain

Some communication systems use orthogonal polarization to isolate between channels. Heavy rainfall will alter the polarization of the transmitted wave by generating an orthogonal component and introduce a cross-polarized component, which may disrupt system performance. Fig. 2(b) and 2(c) show large raindrops that are oblate-spherical in shape, flattened at the bottom, falling with their major axis almost horizontal at various canting angles. The horizontal component of the wave will be more attenuated when it propagates through the rain. In Fig. 3 are the horizontal and vertical components of the resolved radio wave, and the consequent change in its polarization [8].

As two orthogonal vectors E_1 and E_2 propagate the rain filled medium in Fig. 4, the cross polarisation of each vector towards the other component occurs. As such, power is transferred from desired polarization state to the undesired

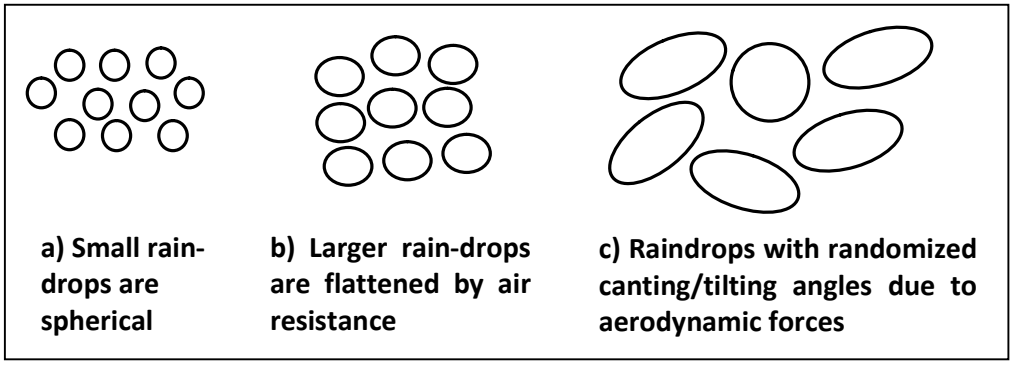

Fig. 2. Variation in raindrop size, shape and angle during rain events [6]

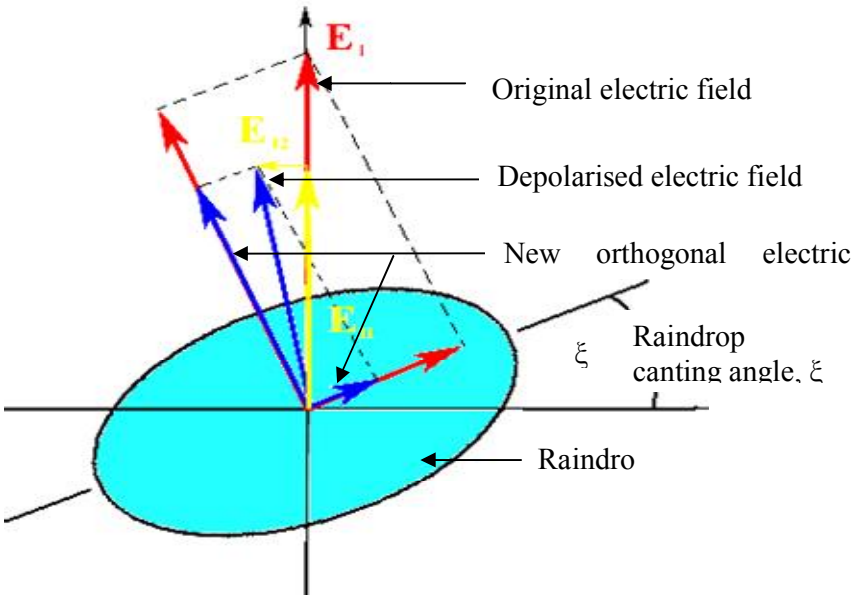

Fig. 3. Depolarization of signal E_1, through an oblate shaped raindrop [8]

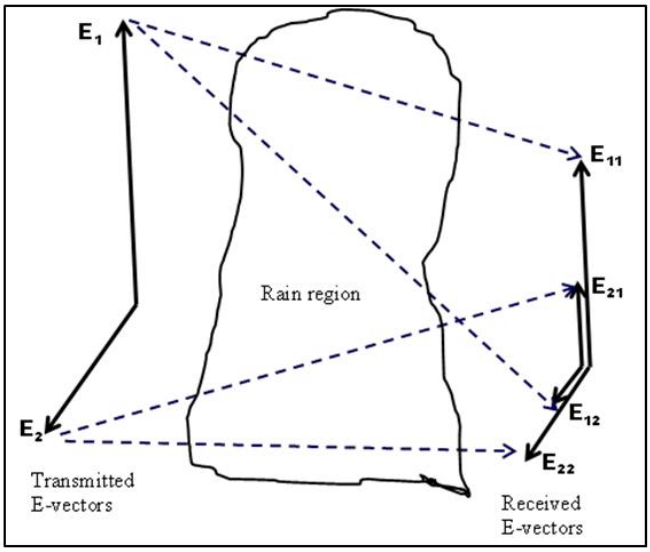

Fig. 4. Cross-polarization of radio-waves due to depolarization through a rain region

orthogonal polarization state, resulting in interference and crosstalk. Depolarisation degradations such as crosstalk and interference are most common with horizontal and circular polarization, because of the differential attenuation and differential phase shift experienced with non-spherical raindrops along the radio path.

Equations describing cross polarization discrimination (XPD) are derived from the power ratio of the wanted (co-polar component, E_{11}) to the unwanted (cross-polarized component, E_{12}). This is defined mathematically as:

$$XPD = 20\log_{10}\left|\frac{E_{co}}{E_{cross}}\right| = 20\log_{10}\left|\frac{E_{11}}{E_{12}}\right| \quad (2)$$

With respect to the co-planar attenuation, the cross-polarization discrimination may be expressed in terms of the radio-path dependent parameters U and V:

$$XPD = U - V \log A \quad (3)$$

where U and V are dependent on frequency, *f*, elevation angle, θ, and canting angle, ξ as indicated in Fig. 3. XPD is evaluated for both horizontal and vertical polarizations.

$$XPD_H = 20 \log \left[\frac{(1-G)\tan\vartheta}{G+\tan^2\vartheta}\right] \quad (4)$$

$$XPD_V = 20 \log \left[\frac{(1+G)\tan\vartheta}{1+G+\tan^2\vartheta}\right] \quad (5)$$

where ϑ is the canting angle and *G* is the differential propagation factor for terrestrial and satellite links are defined as:

$$G = \begin{cases} exp[-(\Delta A + j\Delta\varphi)L \times \cos^2\theta]; & terrestrial \\ exp\left[-(\Delta A + j\Delta\varphi)L \times \frac{1}{2} \times (e^{-2\sigma'^2}\cos 2\theta)e^{-2\sigma^2}\right]; & satellite \end{cases} \quad (6)$$

where *θ* is the elevation angle of the signal, which is 0° for terrestrial; σ is the standard deviation of the angles; and *σ* is the standard deviation of the canting angles, which is 0° for terrestrial and 10° for satellite paths. The symbols ΔA and $\Delta\varphi$ are differential attenuation and phase shift and defined by [12] as:

$$\Delta A = A_H - A_V \quad (7)$$

$$\Delta\varphi = \varphi_H - \varphi_V \quad (8)$$

Radio propagation equipment required for empirical determination of these phase shifts, scattering and attenuation parameters are not readily available. However, [2] derived equations to compute cross polarization discrimination (XPD) from rain attenuation, which was expressed as:

$$XPD = U - V log_{10}(A) dB \quad (9)$$

Where,

$$U = 30\log(f) - 40\log(cos\theta) - 10log\,{}^1/_2\,(1 - cos(4T))e_m^{-k^2} \quad (10)$$

and θ is the satellite elevation angle, T is the local polarization tilt angle, k_m^2 relates to the variance, σ of the canting angle distribution ($k_m^2 = 0.0024\,\sigma_m^2$). Equations (2 to 10) are similar to the procedure prescribed by ITU-R [14] for computing rain XPD for circular, vertical and horizontal polarizations of transmitted waves. The ITU-R [14] procedure was therefore used to compute the rain XPD in the region.

3. EXPERIMENTAL SITE AND METHODOLOGY

The measurement taken at experimental sites are described in [3]. Table 1 presents the characteristics of the experimental site and the parameters for the Ku-band satellite receiver at the location. The experimental set up was used to concurrently measure and record rain-rate, rain attenuation, signal loss, at the location. The rainfall rates were used to formulate models that relate the distribution of rainfall intensities to the impairments caused by rain depolarisation on line of sight (LOS) satellite links in Jos, a Guinea Savanna location in Nigeria.

3.1 Procedure for XPD Calculation [14]

Parameters needed to calculate long-term statistics of depolarization from rain attenuation statistics include:-

- *Ap*: rain attenuation (dB) exceeded the required percentage of the time, *p*, for the path in question, commonly called co-polar attenuation (CPA)
- τ: tilt angle of the linearly polarized electric field vector with respect to the horizontal (for horizontal, vertical and circular polarizations use τ = 0°, 90° and 45°, respectively)
- *f*: frequency (GHz)
- θ: path elevation angle (degrees).

ITU-R in [14] used five basic components to be computed to arrive at the value of XPD due to rain as expressed by equation (11). These include frequency-dependent factor C_f, attenuation factor C_A, polarization factor C_τ, elevation factor C_θ and canting angle factor C_σ.

Rain XPD not exceeded for *p*% of the time is given as:

$$XPD_{rain} = C_f - C_A + C_\tau + C_\theta + C_\sigma \text{ dB} \quad (11)$$

where, the frequency-dependent term is:

$$C_f = 26 \log f + 4.1 \quad \text{for } 9 \le f \le 36 \text{ GHz} \quad (12)$$

The rain attenuation dependent term is:

$$CA = V(f) \log Ap \quad (13)$$

where,

$V(f) = 12.8\, f^{0.19}$, for $9 \le f \le 20$ GHz

Table 1. Characteristics of the experimental site and specification of parameter for the Ku-band link

Measurement site	Gold and Base, Jos, Plateau state (9.9565° N, 8.8583° E; 1258 meters)
Climate region of the site	Guinea Savanna
Max / Ave / Min Temperatures	29.8°C / 22.8°C / 07°C
Satellite Name/ Number	Eutelsalat; W4/ W7 (DSTV Multi-choice)
Satellite signal frequency / Polarization	12.245GHz / Horizontal
Symbol rate	27, 509bps
satellite elevation (orbital)	036E
Satellite Geo-station Lookup	056.5E
Antenna diameter	90cm
Rain Equipment / Integration time	Davis Vantage Vue Integrated Sensor Suite (ISS) weather station and Weather Link

Polarization improvement factor is:

$$C\tau = -10 \log [1 - 0.484 (1 + \cos 4\tau)] \quad (14)$$

Where, $C\tau = 0$ for circular polarization and reaches a maximum value of 15 dB for horizontal and vertical polarizations respectively. The elevation angle-dependent term is:

$$C\theta = -40 \log (\cos \theta) \quad \text{for } \theta \leq 60^{o} \quad (15)$$

The canting angle dependent term is:

$$C\sigma = 0.0052\ \sigma 2 \quad (16)$$

Where σ is the effective standard deviation of the raindrop canting angle distribution, expressed in degrees; σ takes the value 0°, 5°, 10° and 15° for 1%, 0.1%, 0.01% and 0.001% of the time, respectively.

4. RESULTS AND DISCUSSION

Fig. 5 presents the cumulative distribution of one-minute rain rate over Jos (September 2013 – September 2017). It can clearly be seen that the higher rainfall intensities occur between for 0.01 and 0.001% and it is during such times that maximum attenuation due to rainfall can be best estimated. Also Fig. 5 indicates that the distribution of rainfall intensities, R_p at a specified percentage of the time, *p%* could be adequately modelled with a logarithm expression in equation (17) having an agreement factor of 98%:

$$R_p = -22.3 \ln(\mathrm{p}) - 7.75 \quad (17)$$

On the other hand, modelling rainfall intensities with the power law model produced a lower agreement factor of about 91%.

Fig. 6 shows the variation of the XPD with rain attenuation exceeded for the required period of time, often called the co-polar attenuation over the elevation angle at 12.245 GHz. The cross polarization discrimination degrades with increasing co-polar attenuation. The logarithm model in Fig. 6 clearly shows that the signal degradation as a result of XPD is more enhanced by CPA for given fade as seen in the negative slope (or coefficient = -123) of degradation.

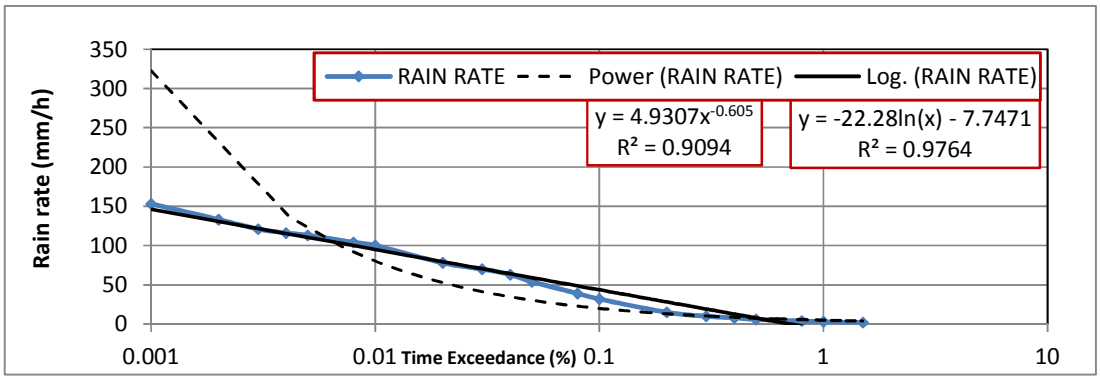

Fig. 5. Distribution of rainfall intensities in Jos

$$XPD_{rain} = -123\ln(A_p) + 213 \quad (18)$$

When

$$XPD_{rain} = 0, \qquad A_p = e^{1.73} = 5.6\ dB \quad (19)$$

Since the relationship between XPD_{rain} and CPA has a perfect correlation of $R^2 = 1$, equation (18) could be used as a perfect model for deriving rain induced XPD at any given level of attenuation in the region.

Equation (19) indicates that XPD_{rain} will be completely degraded to zero, when the co-polar attenuation reaches 5.6 dB in the location. This means that the amount unwanted cross polarized signals equals the wanted signal and the signal is completely overshadowed by interfering signals and crosstalk within the orthogonal frequency band. This scenario creates undesirable degradation in the channel that demand for the development of mitigation techniques.

Also, Fig. 6 shows negative values of rain-induced XPD for attenuation values above 5.6 dB. This implies that the values of unwanted cross-polarized signals, (interference and crosstalk) are higher than the level of the desired signal. At such instances, only the crosstalk and interferences are received at the receiver station of the satellite link. It is desirable to develop mitigation techniques to arrest such degradation.

Fig. 7 shows the variation of XPD with rain rate at 12.245 GHz. As rain rate increases, XPD decreases. This results in very high interference level in the orthogonal channels. A relation was observed between the XPD and rain rate, which showed an almost perfect fit of 99%, as seen in logarithm expression in equation (20):

$$XPD_{rain} = -75\ln(R_p) + 246\,, \quad R^2 = 0.99 \quad (20)$$

When

$$XPD_{rain} = 0, \qquad R_p = e^{3.28} = 26.6 \text{ mm/h} \quad (21)$$

The implication of equation (21) is that when rainfall intensities of about 27 mm/h, interferences and crosstalk become prevalent at the receiver end of the Ku-link and communication is completely impaired. Mitigation techniques must therefore be implemented to cater to cross-polarization defects and improve throughputs of the link.

Considering the temporal distribution of cross-polarization over Jos, Fig. 8 shows that all percentages of time above 0.1% experience positive cross polarization, while all finer percentages of time below 0.1% experience negative cross-polarization. As explained earlier, a negative value of XPD means that unwanted interference and crosstalk are prevalence in the region. The operations of most satellite links are significant at finer time percentages between 0.05 and 0.001 for acceptable quality of service, but this is the period when degradation (crosstalk and interference) is most prevalent. Thus, in the Guinea Savanna region of Nigeria, it is difficult to optimize the channel capacity of radio links through frequency re-use by deploying dual independent orthogonally polarized channels in the same frequency band.

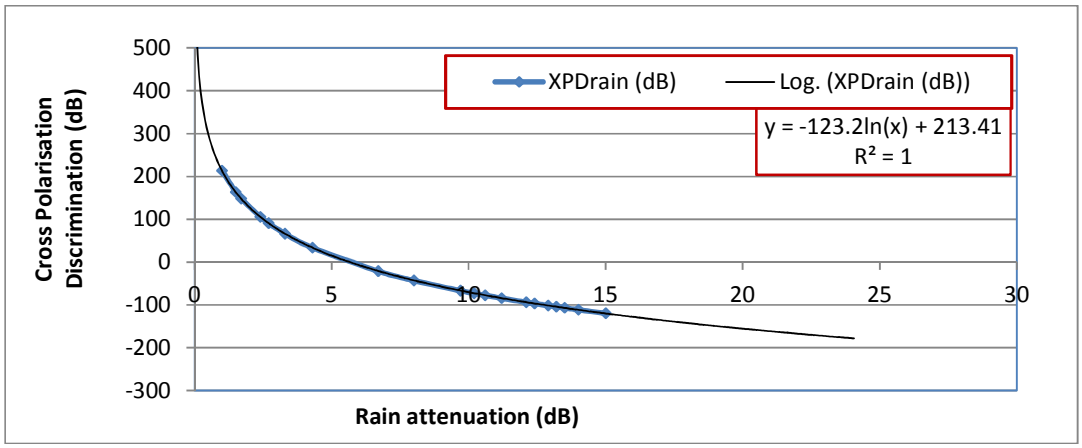

Fig. 6. Variation of cross polarization discrimination (XPD) with rain attenuation (C_A)

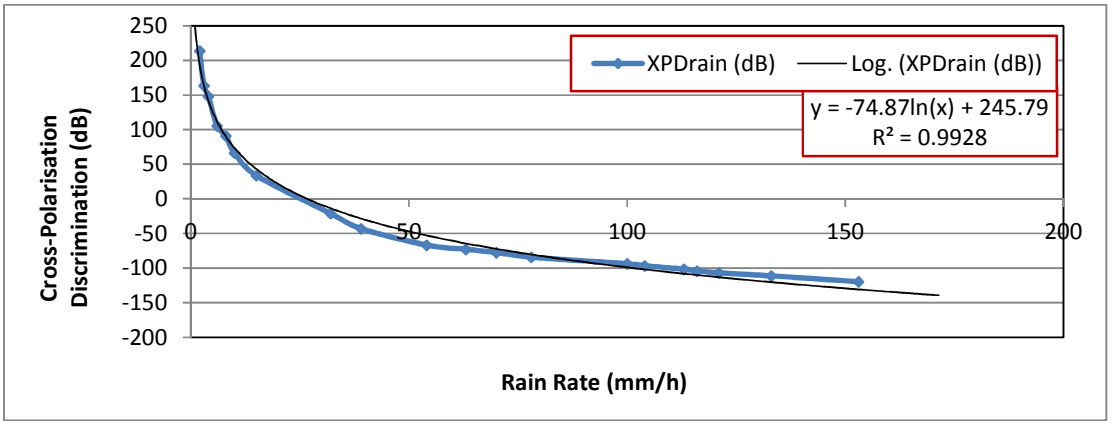

Fig. 7. Variation of cross polarization discrimination (XPD) with rain rate

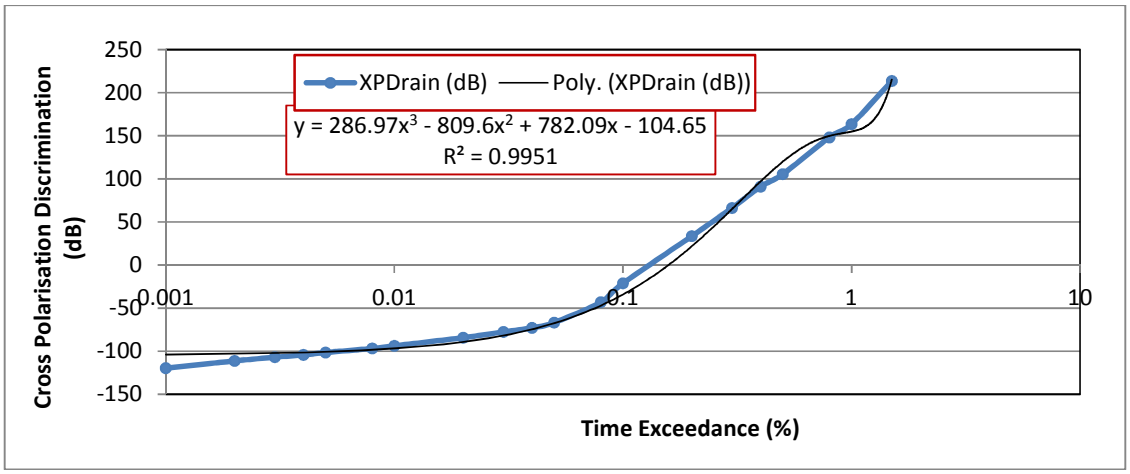

Fig. 8. Temporal distribution of cross polarization discrimination (XPD) over Jos

5. CONCLUSION

This paper presents some features of propagation phenomena observed with a Ku-band signal over Jos – a Guinea Savannah location in Nigeria. These data were applied to the ITU-R procedures in recommendation 618-12 [14] to estimate the cross polarization discrimination due to rain on earth satellite path. From the results, simple logarithm equations were derived to relate XPD to rain rates, rain attenuation and percentages of time. Threshold of rain rate for positive values of XPD was 37 mm/h, while the threshold for co-polar attenuation was found to be 6.7 dB. These values are useful for radio communication planning in the region. Finally, results obtained show that negative values of XPD value of about -120 dB imply very high incidences and cross talks are prevalent in the region. As such frequency re-use is difficult in Guinea Savanna region of Nigeria. However, the findings and simple logarithmic models in this study provide useful considerations to guide telecommunication operators in infrastructure planning and design. Service providers may use the models to formulate infrastructure and investments policies to optimize the current scenario of frequency re-use.

COMPETING INTERESTS

Authors have declared that no competing interests exist.

REFERENCES

1. Kaustav C, Animesh M. Depolarization of Ku-band satellite signal in relation to rain attenuation for the tropical region. S.K

Mitra Centre for Research in Space Environment, Institute of Radio Physics and Electronics, University of Calcutta, Kolkata 700009, India; 2011.
2. Muhammed Z, Zaffar H, Shahid AK, Jamal N. Atmospheric influences on satellite communications. COSATS, Institute of Information Technology, Islamabad Abbott Abad. 2011;4:261-264.
3. Durodola OM, Ojo JS, Ajewole MO. Performance of Ku-band satellite signals received during rainy condition in two low-latitude tropical locations in Nigeria. Adamawa State University Journal of Scientific Research. 2017;5(1). Available:http//www.adsujsr.com
4. Oguchi T. Scattering properties of oblate raindrops and cross polarization of radio waves due to rain, calculation at 19.3 and 34.8 GH_Z. Journal Radio Resources Laboratory Japan. 1994;20(102):79-118.
5. Ajewole MO, Kolawole LB, Ajayi GO. Cross polarization on line-of-sight links in a tropical location: Effects of the variation in canting angle and raindrop size distributions. Antennas and Propagation, IEEE Transactions. 1999;47(8):1254-1259.
6. Roddy D. Satellite communications, 4th edition. McGraw-Hill Companies, Inc. New-York; 2006.
7. Garg K, Nayar SK. Photometric model of a rain drop. Technical Report, Columbia University; 2003.
8. Rytir M. Radiowave propagation at Ka-band (20/30 GHz) for satellite communication in high-latitude regions; being Masters thesis in Electronics, submitted to the Department of Electronics and Telecommunications, Norwegian Univ. of Science and Tech. (NTNU) Trondheim, Norway; 2009.
9. Animesh M, Arpita A. Ku-band signal depolarization over earth – space path in relation to scattering of raindrops at a tropical location. S.K Mitra Centre for Research in Space Environment, Institute of Radio Physics and Electronics, University of Calcutta, Kolkata 700009, India; 2011.
10. Appolito LJ. Radio propagation for space communication systems. In Proceedings of the IEEE. 1981;69(6).
11. Oguchi T. Attenuation and phase rotation of radio waves due to rain: Calculation at 19.3 and 34.8 GHz. Radio Science. 1973;8(1):31–38.
12. Ajewole MO. Scattering and attenuation of centimetre and millimetre radio signals by tropical rainfall. Doctoral Dissertation, Federal University of Technology, Akure, Nigeria; 1997.
13. Senzo JM. Determination of millimetric signal attenuation due to rain using rain rate and raindrop size distribution models for Southern Africa. PhD Thesis (Electronics Engineering) University of Kwa-Zulu-Natal (UKZN), Durban South Africa; 2014.
14. ITU-R Recommendation P.618-12: Propagation data and prediction methods required for the design of Earth-space telecommunication. Geneva; 2015.

© 2018 Durodola et al.; This is an Open Access article distributed under the terms of the Creative Commons Attribution License (http://creativecommons.org/licenses/by/4.0), which permits unrestricted use, distribution, and reproduction in any medium, provided the original work is properly cited.

Peer-review history:
The peer review history for this paper can be accessed here:
http://www.sciencedomain.org/review-history/23689